Vol. 48 No. 1 Journal of the Communications Research Laboratory March 2001
Printed in Tokyo, Japan pp. 31−40

2.5 Stellar Evolution and Water Maser Emission

By
Hiroshi IMAI

ABSTRACT

Cosmic maser emission from water vapors has been observed at an early stage of birth and at the final stage of death in stellar evolution. We have observed such water masers using the Japanese domestic VLBI network for astronomy (J-Net) and revealed in detail the kinematics of water masers around protostars and evolved stars. The results of these observations are summarized as follows. (1) Systematic radial-velocity drifts of water maser features with time were found around the semiregular variable star RT Vir. This phenomenon, first discovered here, indicates acceleration motion of mass-loss flow around the star. (2) Rotation-infall motions around the protostar IRAS 16923-2422 were revealed on a solar-system scale with water masers. These motions indicate a dynamical infall of materials onto the protostar on a scale down to a few tens of AU. (3) A large number of proper motions of water maser features were measured in the massive-star forming region W51 North. The 3D kinematics of an outflow from W51 North was determined and the distance to W51 North was estimated directly as 6.7±2.1 kpc. (4) A study of high precision astrometry for maser sources was begun to advance stellar astrophysics. In this study, the phase-referencing technique by a fast antenna-switching method was applied to water masers around the supergiant star S Per and the continuum source KR 143. Although the accuracy of relative astrometry for the maser sources is limited to 1 mas at present, fringe-phase fluctuation due to the atmosphere can be compensated effectively in a relatively high frequency band of 22.2 GHz.

Keywords: Water masers, Very long baseline interferometry, Star formation, Evolved stars, Astrometry

1. Overview

Water masers around stars can be observed during energetic mass ejection at the early and late stages in a stellar evolution corresponding to the star's birth and death. We have observed such water masers using the Japanese domestic VLBI network for radio astronomy called "J-Net" and have achieved the following results. (1) Systematic radial-velocity drifts were detected in individual maser spots with time around the pulsating variable star (semiregular variable star) RT Vir. (2) Water-masers were discovered around the protostar IRAS 16923-2422 in gases exhibiting rotation-infall motions on a solar-system scale. (3) Relative proper motions were observed among maser features in the massive-star forming region W51 North, and estimations of the 3D kinematics of gas in this region and the distance to W51 North were made directly. Trials of the differential VLBI observations for water-maser sources were also performed in anticipation of future advances in this research field. (4) The differential VLBI observations based on fast antenna switching (switching period: 60 seconds) were performed on J-Net for water masers around the supergiant star S Per and the nearby continuum source KR 143, and feasibility of this observation technique was demonstrated.

2. Stellar Evolution and Water Masers

At the early stage of star formation, gas falls inward in the core of a molecular cloud, the "womb" of a protostar, and some of this gas is ejected from the protostar and its immediate area in the form of a jet or a molecular outflow. Such an energetic ejection of gas also occurs at the last stage of stellar evolution, that is, the asymptotic giant branch (AGB) stage corresponding to the formation of planetary nebula from a Mira variable star. While the mechanisms that drive these three phenomena and that greatly affect stellar evolution differ from each other, it is extremely important that the motion of gas associated with the phenomena be well understood in order to elucidate those mechanisms. The spatial scale in which these phenomena occur, however, covers a wide range. In particular, it is not trivial to obtain information on motion in a region having an extremely small field of view near a protostar or pulsating variable star due to the spatial resolution limits of observation equipment. Under these circumstances, VLBI observations of water masers are especially suitable for this purpose described as follows.

A water-maser source consists of a group of maser features that have various positions and velocities and that are distributed in very vicinity of protostars and pulsating variable stars where the physical processes described above occur. Individual features, moreover, are extremely compact (typically 1 AU). The only way to spatially isolate such a feature is VLBI. At present, the spatial resolution achieved by VLBI is typically one milliarc second, and a precision of one microarc second can be achieved through relative position measurements between features. Making full use of this spatial resolution and precision in position measurements makes it possible to obtain considerable information on the kinematics of the above physical processes.

In the following sections, we will present new information on the kinematics of water masers associated with star-forming regions and evolved stars obtained

through observations using the Japanese domestic VLBI network (J-Net). We note, however, that the kinematics described below are relative to a specific maser feature as a position reference. This means that we lack important observational quantities such as precise absolute positions on the celestial frame and an overall motion of maser sources. In this regard, "the differential VLBI" has been attracting attention as a means of obtaining such information, and we also report here on efforts to put this technique into practice on J-Net.

3. Research of Stellar Physics through J-Net VLBI Observations

3.1 J-Net observations, correlation processing, and data analysis

The J-Net consists of four radio telescopes in total. These are the 10-m antenna at Mizusawa, the 45-m antenna at Nobeyama, and the 6-m antenna at Kagoshima belonging to the National Astronomical Observatory (NAO) and the 34-m antenna at Kashima belonging to the Communications Research Laboratory (CRL)[1]. The emission lines of water masers exist in the 22.2-GHz band, and the minimum fringe interval in this band is 2.1 milliarc seconds. For the backend here, the K-4 terminal was used up until September 1997[2] and the VSOP terminal has been used since then[3]. Table 1 shows specifications of the K-4 and VSOP terminals.

The observation data handled by the author were obtained by subjecting recorded signals from K-4 and VSOP terminals to correlation processing by the New Advanced One-unit Correlator (NAOCO)[4] and the Mitaka FX Correlator[5], respectively. The correlation output from NAOCO was fixed at 256 frequency channels per 1-sec integrating period (parameter period) and baseband channel. With the FX Correlator, both bandwidth and number of spectral channels could be changed from one observation to another. These output data from NAOCO and the FX correlator were employed for calibration and image synthesis using the fringe-rate mapping software developed in-house and the Astronomical Image Processing System (AIPS), respectively.

3.2 VLBI monitoring observations of water masers around the semiregular variable star RT Vir

Monitoring observations of water masers around RT Vir by J-Net were performed five times in the period from February to May 1995 (see Table 2). In these observations, the accuracy for determining relative positions in the fringe-rate mapping was 15 milliarc seconds for right ascension and 50 milliarc seconds for declination, which was not sufficient for measuring the relative proper motions of maser spots. The following two important results, however, could be obtained[6].

The first result was detection for the first time of systematic radial-velocity drifts in individual maser features with time (left graph in Fig. 1). This detection was made possible by the high velocity resolution (0.1 km s^{-1}) of NAOCO correlation-processing output. The spatial distribution of maser spots for which radial-velocity drifts were detected is shown in the right graph of Fig. 1. The measured radial-velocity drift rates were in the range from -3.6 to 1.8 km $s^{-1}yr^{-1}$. We note here that gas around a pulsating variable star is accelerated outward by radiative pressure from the star, which is received interstellar dust in the gas. The magnitude by observed radial-velocity drifts, moreover, can be surmised from a theoretical model and the observed expansion velocity increasing with the distance from the star. Note that the theoretical model supports the occurrence of shock waves

Table 1 Specifications of K-4 and VSOP terminals used by J-Net

	K-4 Terminal	VSOP Terminal
Recording rate	64 Mbps fixed	64,128 or 256 Mbps
No. of quantization bits	1 bit/sample	2 bits/sample
Baseband channels	2 MHz×16	16 MHz×1 or 2 32 MHz×1 or 2

Table 2 Monitor observations of water masers around RT Vir by J-Net (1995)

Observation Code	Observation Date	Total Observation Time	Participating Stations[1]
d95017	January 17	—[2]	M, k
d95050	February 21	8 hr	M, k
d95058	February 28	8 hr	M, b[3], k
d95095	April 6	8 hr	M, b[3], n[4], k
d95129	May 9	8 hr	M, b[3], n[4], k

[1]M: Mizusawa 10-m antenna, b: Kashima 34-m antenna, n: Nobeyama 45-m antenna, k: Kagoshima 6-m antenna
[2]Snapshot observation (two 6-minute scans)
[3]Effective drop in efficiency (about 10%)
[4]Rise in system noise temperature (240-290 K)

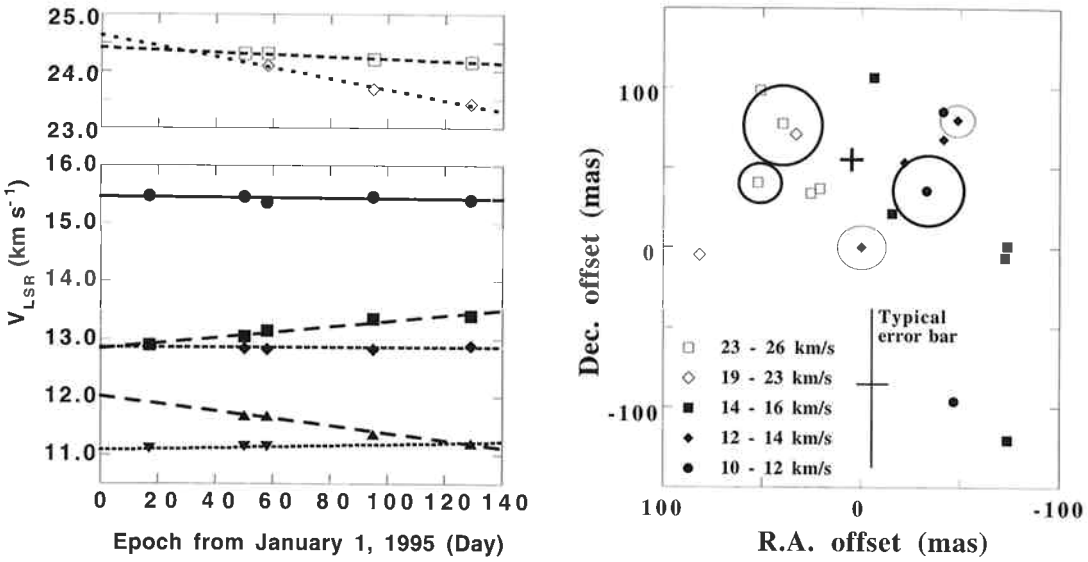

Fig. 1 Graphs on water masers around the semiregular variable star RT Vir
Left graph: Systematic radial-velocity drifts of water maser features.
Right graph: Spatial distribution of radial velocity of water maser features. The distribution for April 1995 is shown. The circles enclosing maser features indicate radial-velocity drift. The thick and thin lines indicate radial-velocity drift toward a blue shift and red shift, respectively, and circle radius is proportional to drift rate.

and the rapid acceleration/deceleration of peripheral gas due to pulsating light, and a greater magnitude is expected in this case for radial-velocity drift. However, as no correlation is observed here between relative position and radial-velocity drift; it is still unclear whether this radial-velocity drift actually indicates true accelerated motion of the gas.

Next, from the date of the previous and present observations for 10 years, correlation was found between the extension of the maser-spot spatial distribution and the pulsating light curve. Because RT Vir is a semiregular variable star, its pulsation period and phase are unclear. For this reason, the light curve was estimated using the phase-dispersion minimization method and the pulsation period was determined to be about 360 days. It was also found that the maximum brightness period and maximum period of maser-distribution extension were offset by a half cycle, and that each varies periodically. These findings provide indirect proof that the shock wave created by pulsating light propagates outward and excites water masers.

3.3 VLBI observations of water masers around the protostar IRAS 16293-2422

Direct observations of contraction of a molecular-cloud core and mass infall toward a protostar began toward water maser sources in the 1990's. Before then, only water masers associated with outflow in star-forming regions had been confirmed. A water maser source associated with a mass-accretion gas disk was finally discovered in 1996[7]. There have been other examples of water-maser sources associated with gas disks or tori. These sources do not indicate infall motions, except only two sources including an example presented here by the author.

The example of a water-maser source associated with an accretion disk is the one around IRAS 16293-2422. This water maser source was observed in 1991 using the Kashima Nobeyama InterFErometer (KNIFE) and in April and May 1994 using the four J-Net stations (see Refs. (8) and (9) and Table 3). Here, analysis by the fringe-rate mapping was able to achieve maser maps at a measurement accuracy of 10 milliarc second with respect to relative positions between maser features. IRAS 16923-2422 is a low-mass (0.3 $M_{\odot}$) star. Generally speaking, the lifetime of water maser spots associated with these stars are thought to be relatively short. Fortunately, although individual features appeared to light up and disappear over the course of the above three observations, the radial-velocity distribution in the entire maser source was quite similar over these observations. This result made it possible to overlay these maser maps and obtain one map, as shown in the left graph of Fig. 2.

Roughly speaking, the distribution of water maser spots stretched in a direction that was nearly perpendicular to the direction of the outflow from the protostar. The structure of its internal radial velocity, however, did not exhibit a simple velocity slope but complex. It was later found that this could be neatly explained by a model of water-maser excitation. In this model, a mass falling toward a gas disk with rotation excites water maser emission when colliding with the disk. A radial-velocity distribution of gas predicted by calculations based on this model is shown overlaid on the left graph of Fig. 2.

Based on this model of gas motion that describes actual observations well, we can see an important issue of gas falling toward the protostar. To clarify, the right graph of Fig. 2 shows the radius dependency of angular

Table 3 Observations of water masers around IRAS 16293-2422 by J-Net

Observation Code	Observation Date	Total Observation Time	Participating Stations[1]
d91148	May 28, 1991	5.5 hr	b, n, U
d94095	April 5, 1994	7.7 hr	M, b, n, k
d94152	June 1, 1994	7.7 hr	M, b, n, k

[1]M: Mizusawa 10-m antenna, b: Kashima 34-m antenna, n: Nobeyama 45-m antenna, k: Kagoshima 6-m antenna, U: Usuda 64-m antenna

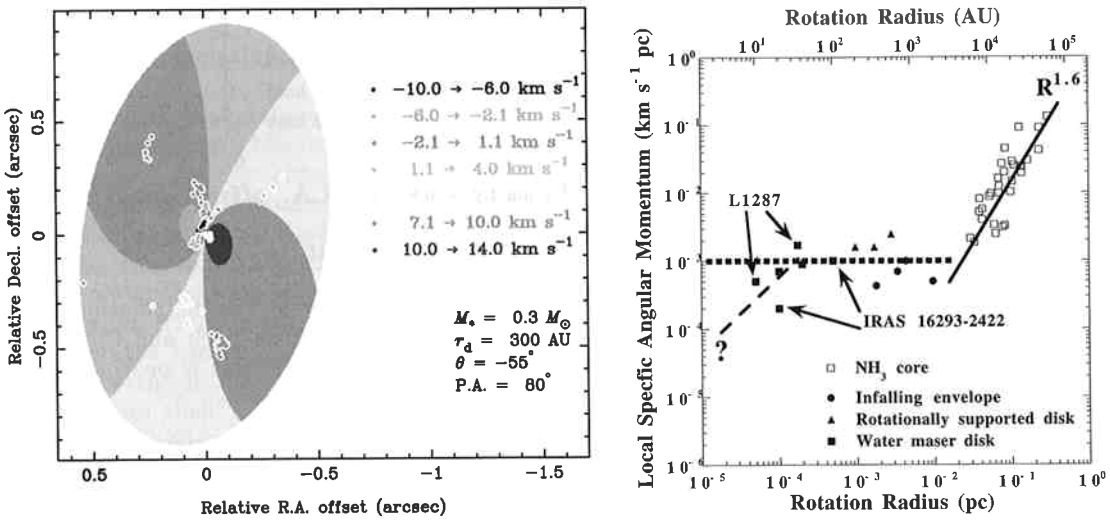

Fig. 2 Graphs on water masers around the protostar IRAS 16923-2422
Left graph: Distribution of maser spots (points) obtained by combining three water-maser maps and radial-velocity distribution (color-coded) on a gas disk as estimated by a model of rotation-infall motion of circumstellar gas. The gas disk shown has a radius of 150 AU. The mass of the protostar at the center of the gas disk as estimated by the model is 0.3 $M_\odot$. The direction of disk rotation axis agrees well with that of the CO-emission-line outflow (a nearly east-west direction: Hirano et al., private correspondence).
Right graph: Radius dependency of local-specific angular momentum observed in protostar gas envelopes, circumstellar gas disks, and water maser disks. The power-law fit of local-specific angular momentum at 0.03 pc or greater and the fixed lines of local-specific angular momentum at a lower scale are from Ohashi et al[10].

momentum per unit mass (local-specific angular momentum). It is know that the molecular cloud core contracts inward while loosing angular momentum at distances beyond a radius of 0.03 pc from the protostar, but that within this radius it undergoes a type of free-fall motion (dynamical infalls) while preserving its local-specific angular momentum[10]. For the gas disk associated with the IRAS 16293-2422 water maser observed by J-Net, such dynamical infalls can be seen down to a scale of 10 AU from the protostar. The issue in future VLBI observations is to explain gas motion within 10 AU from the protostar.

3.4 Observations of proper motions among maser features in the massive-star forming region W51 North

With the use of AIPS to perform data analysis, the accuracy of measurements taken of the relative positions of water-maser features through J-Net observations is improved to typically 0.1-0.2 milliarc second. The first proper motions among maser features were consequently measured by J-Net in 1998[11].

Then, in 1999, similar proper motions were measured in the massive-star forming region W51 North (see Ref. (12), Table 4). In this case, three water-maser sources (W51 North, Main, and South) exist within 60 arc seconds. As a result, the sources were actually observed within the single beam field of telescopes. In addition, a phase-tracking center was set for each maser source and correlation processing was performed a total of four times. The following describes only the observation results obtained for the W51 North water maser.

In the W51 North region, it took at least two observations to detect more than 100 maser spots and to measure their proper motions. The maser maps obtained from five observing sessions were overlaid by using the position-reference fature, which had simple and compact

brightness distribution and was detected in all of the observing sessions. Part of these relative position changes (relative proper motions) obtained through actual measurements are shown in the left graph of Fig. 3. Many instances of large proper motion exceeding 3 mas yr^{-1} (equivalent to 100 km s^{-1} assuming that the distance to W51 is 7 kpc) were detected. Information on 3D kinematics was also obtained from the radial velocities and proper motions, as shown in the right graph of Fig. 3. Measurements of proper motions among maser features in this region were also performed by Schneps et al.[13], but the number of proper-motion measurements performed at that time came to only 31. It was possible to make many more proper-motion measurements here and to obtain a clear illustration of the outflow in this region for the first time.

At first glance, the W51 North outflow appears to be bipolar. However, the results of velocity-field analysis by a least-square model assuming a spherically symmetric velocity field tell us that chaotic motion dominates. Figure 4 shows expanding flow velocity versus distance from the protostar. Here, practically no dependency on distance (such as for acceleration) can be observed—gas is shown to be flying out at various expanding velocities but at an average of 70 km s^{-1}. On the other hand, water-maser flows found in early-stage masers or intermediate/low mass protostars are more collimated and it can be surmised that the structure of flow depends on stage in star-formation process or the mass of the protostar. Applying this sort of analysis to maser sources in various star-forming regions can clarify a star's stage in star-formation process and how its flow will develop.

One of the most important results of these observations was direct determination of the distance to W51

Table 4 Observations of water masers in W51 by J-Net (1999)

Observation Code	Observation Date	Total Observation Time	Participating Stations[1]	Detection Limit (Jy/beam)	Synthesized Beam[2]
j99052	February 21	11 hr	M, b, k	9.3	7.4×2.4, −38.4°
j99092	April 2	10 hr	M, b, n[3], k	3.8	8.8×2.9, −51.6°
j99126	May 6	10 hr	M, b, n, k	2.9	8.1×3.0, −41.3°
j99157	June 6	10 hr	M[5], b[4,5], n[5], k[5]	4.0	7.2×2.6, −54.2°
j99294	October 21	11 hr	M, b, k	22	7.6×2.4, −38.2°

[1]M: Mizusawa 10-m antenna, b: Kashima 34-m antenna, n: Nobeyama 45-m antenna, k: Kagoshima 6-m antenna
[2]Major axis × minor axis (milliarc sec), azimuth angle
[3]Terminated after 7 hours due to wind
[4]Backend problems
[5]Rise in system noise temperature due to rain

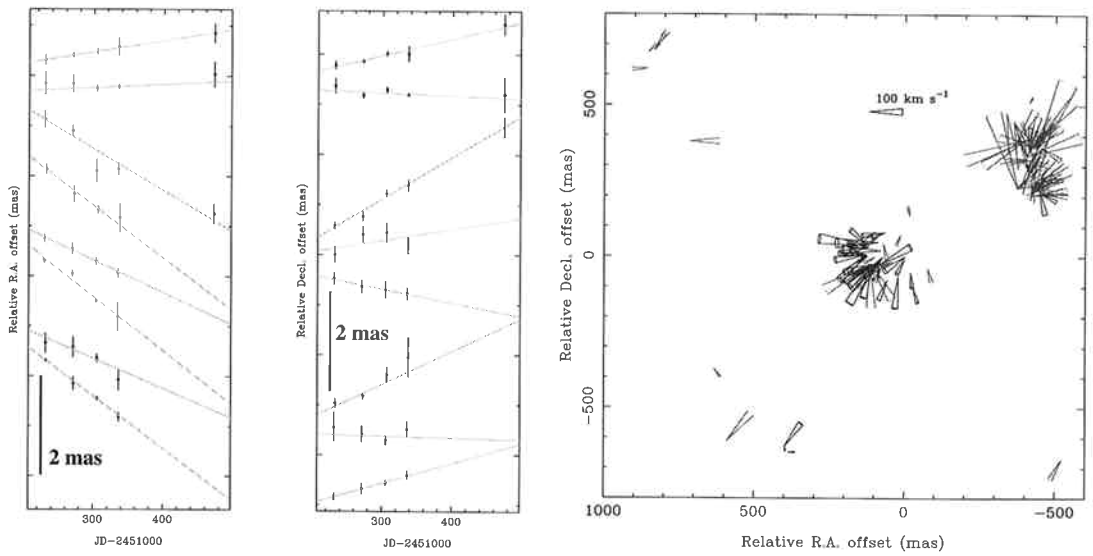

Fig. 3 Measurements of relative proper motions of maser features in the massive-star forming region W51 North
Left graph: Change in relative position over time of maser spots detected four or more times (points with error bar attached) and proper-motion fit (straight line).
Right graph: Relative 3D motion of the W51 North region obtained from proper-motion and radial-velocity information. Maser features exist at the top of the cone and move in the direction of the extending cone.

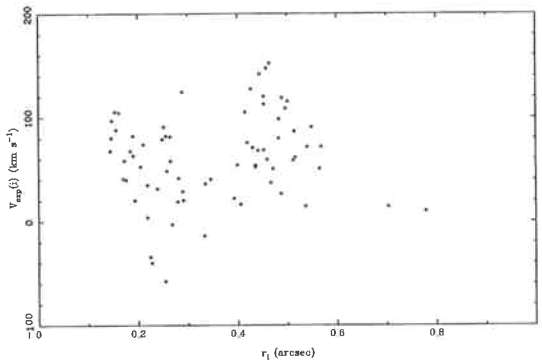

Fig. 4 Plot showing dependency of maser-feature expansion velocity in the W51 North region on distance from estimated position of the massive star. A model fit was obtained from 3D motion data.

North with good accuracy. At present, methods for making direct measurements of the distance to star-forming regions or molecular clouds are only those that use water maser sources, and to date, the number of celestial objects measured their distance in this way is only ten. In this measurement for W51 North, distance was estimated using both the statistical parallax and model-fit methods.

The statistical parallax method compares radial-velocity variance and proper-motion variance assuming that gas motion is isotropic and chaotic. Denoting the standard deviation (square root of variance) of observed radial velocity and proper motion as σ_{vrad} and σ_μ, respectively, the following relationship holds in terms of D, the distance to the celestial object in question.

$$\sigma_\mu = \frac{\sigma_{vrad}}{D},\ \sigma_\mu^2 = \sigma_{\mu,obs}^2 - \sigma_{\mu,err}^2 \quad \cdots\cdots (1)$$

Here, $\sigma_{\mu,obs}$ and $\sigma_{\mu,err}$ are standard deviation in observed proper motion and error in proper-motion measurement, respectively. This error in proper-motion measurement results in an underestimate of distance, which must be corrected.

The model-fit method searches for a distance and a motion model that best fits observed 3D motion. This method uses, in particular, the following non-linear least-squares method.

$$S^2 = \frac{1}{3N_m - N_p} \times \sum_i \left\{ \frac{[\mu_{ix} - w_{ix}/(a_0 d)]^2}{\sigma_{ix}^2} + \frac{[\mu_{iy} - w_{iy}/(a_0 d)]^2}{\sigma_{iy}^2} + \frac{[u_{iz} - w_{iz}]^2}{\sigma_{iz}^2} \right\} \quad \cdots\cdots (2)$$

N_m: Number of 3D motion measurements
N_p: Number of free parameters
$(\mu_{ix}, \mu_{iy}, \mu_{iz})$, $(\sigma_{ix}, \sigma_{iy}, \sigma_{iz})$: Proper motion and radial velocity, and their error
(w_{ix}, w_{iy}, w_{iz}): Model velocity field (including translational motion)
d: Distance to celestial object
a_0: Conversion constant between proper motion and space velocity

The values for the distance to W51 North estimated by these two methods were 7.2±1.7 kpc and 6.3±1.2 kpc, respectively, This gives an average of 6.7±2.1 kpc, which is roughly equal to the traditionally accepted value (about 7 kpc). At the same time, this average value is consistent with the value of 8.3±2.5 kpc from past statistical parallax measurements[13] and reflects a significant jump in accuracy in the model fitting method.

4. Research of the Differential VLBI Method for Water-Maser Sources

4.1 Problems in conventional maser-source astrometry

The kinematic information obtained from maser-source observations presented above is relative to specific maser spots that provide a positional reference. As a result, important information such as precise absolute positions on the celestial frame and overall motions of maser sources are lost, which are a major loss for stellar physics research. For example, in comparing a stellar position observed by infrared radiation with the distribution of maser spots, accuracy is not that high (about 100 milliarc second). As a result, there is no way of determining how the region in which water masers are excited by the behavior of the star itself is affected. Also, in regard to 3D motion, bipolar flow and unipolar flow cannot be distinguished. From the start, the accuracy in measuring proper motion by overlaying maps is limited to 0.1-0.2 mas depending on the structure of the maser spot that is selected as a position reference. For this reason, more precise measurements of proper motions, and for that matter, detection of accelerated motion in addition to linear motion, are not possible at this time.

"The differential VLBI" is a one method that makes simultaneous or nearly simultaneous observations of two celestial objects that, while near to each other, do not fall into the view of a single telescope. In this way, the relative positions between two celestial objects can be measured with high precision, and the fringe phase of one object can be tracked to detect other weak radio source by long-term coherent integration. This method also makes it possible to perform a high-precision measurement of relative positions between a water-maser source and adjacent distant quasi-stellar object (QSO) as a pair, and to measure absolute position of that maser source on the celestial reference frame with high accuracy.

4.2 Differential VLBI observations by the fast-antenna-switching method targeting the supergiant star S Per and the continuum source KR 143

The differential VLBI observations targeting a maser source using J-Net were first carried out in 1995 by Sasao et al. The present VLBI observations were performed in December 1999 and March 2000 targeting the maser source associated with the supergiant star S Per and the continuum source KR 143 separated by 13'.2 from that maser source. Like the previous differential VLBI observations performed on J-Net, the present observations made use of the fast-antenna-switching method. In this method, two celestial objects cannot be observed simultaneously, but reciprocally by swinging the antenna with a period allowed by fluctuation in fringe

phase caused by the atmosphere. In the 22.2-GHz band, this switching period can be taken to be 60 seconds (under good weather conditions) from a theoretical model of the atmosphere. Table 5 gives the observation status.

Antenna switching in the present VLBI observations was therefore performed in a 60-second cycle: the antenna would scan S Per for 25 seconds, after five seconds for slewing scan KR 143 for another 25 seconds, and five seconds after this scan S Per again for 25 seconds, and so on. The angular separation between these two celestial objects was small, and an observation that could be made without applying a major load on the telescope drive mechanism or the azimuth rail did occur. On the other hand, there were times when the antenna drive could not catch up even with the five-second margin (a loss of almost five seconds) showing the limits of observation by this mode on J-Net. A successful relative VLBI observation was made on only the first epoch under fair skies and a smoothly running observation system.

Figure 5 shows the maps obtained for the S Per water maser and KR 143. For the former, relative proper motions between maser features were also measured between two observations, and these motion are also shown as arrows. The second observation, however, suffered from a drop in sensitivity due to backend problems at the Kashima station and poor weather at Nobeyama. As a result, the number of detected maser spots decreased

Table 5 Relative VLBI observations between S Per water maser and continuum source KR 143

	S Per Water Maser	KR 143
Phase tracking center for correlation processing	$\alpha_{J2000} = 02^h22^m51^s.713$ $\delta_{J2000} = +58°35'11''.44$	$\alpha_{J2000} = 02^h22^m33^s.040$ $\delta_{J2000} = +58°48'12''.77$
Obtained relative position of celestial object[1]	....	$\Delta\alpha = -18^s.19005 \pm 0^s.00007$ $\Delta\delta = +13'02''.4873 \pm 0''.0004$
Bandwidth for correlation processing	4 MHz (baseband center: 12-16 MHz)	32 MHz
No. of spectral channels for correlation processing	256	256
Baselines used in data analysis[2]	n-b, n-M, n-k, M-b	n-b, n-M, M-b
Synthesized beam[3]		
(1999 December 27)	5.3×4.1 mas, P.A.=−84.°3	7.3×7.1 mas, P.A.=−81.°0
(2000 March 12)	6.3×4.1 mas, P.A.=−87.°3	.....

[1]Origin of coordinate system is at a maser spot associated with S Per having radial velocity $V_{LSR} = -46.85$ km s^{-1}.
[2]M: Mizusawa 10-m antenna, b: Kashima 34-m antenna, n: Nobeyama 45-m antenna, k: Kagoshima 6-m antenna
[3]After eliminating tapering and effects of bad visibility

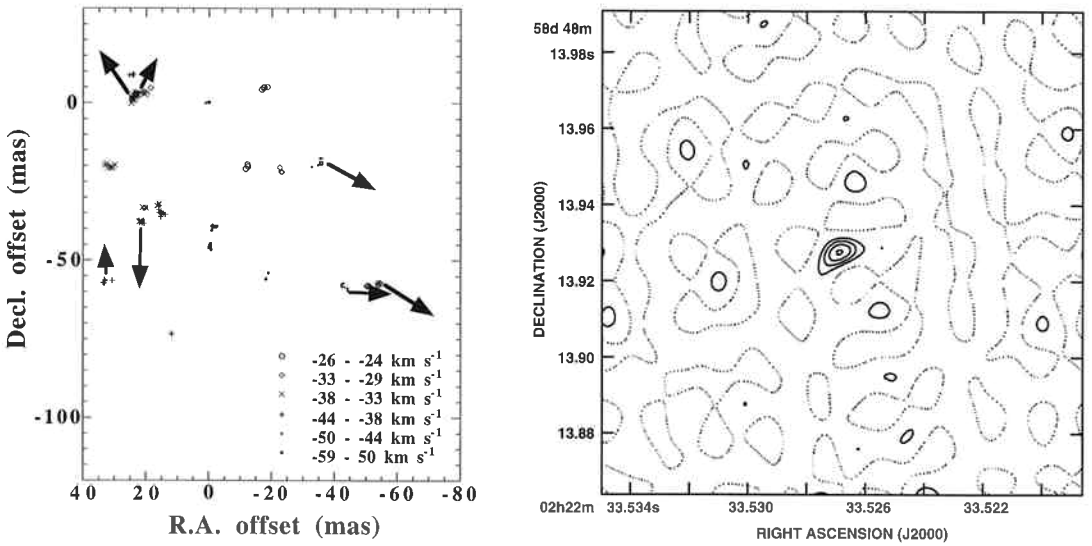

Fig. 5 Left graph: Distribution of maser-features associated with S Per and detected proper motions. Length of arrows represents actual motion enlarged 30 times.
Right graph: Map of radio-source KR 143. Contour levels from the bottom are −1, 6, 9, 12, and 15 mJy. Data was fitted to an elliptic-Gauss brightness distribution, and brightness-peak intensity and flux density were calculated to be 16.5±2.5 mJy/beam and 14.6±4.0 mJy, respectively.

and the number of measured proper motions came to only seven. Nevertheless, it was still possible to come up with a similar expansion motion as found in the previous proper-motion measurements[14].

As for KR 143, we were barely able to detect it with a flux of 15 mJy at a 6-σ noise level. The detected position was offset 4" to the northeast from the initially adopted phase tracking center. This offset, though, is though to be reasonable considering that the accuracy of absolute position measurements by 1.6-GHz observations using a VLAD array, the basis for that initial value, is not that high, and or looking at radio lobes from the core in the 1.6-GHz band is quite possible.

4.3 Discussion of the differential VLBI observations

Table 6 gives the sources of error in measurements of relative positions between two celestial objects. The main contribution to this error is error in the baseline vector between Nobeyama and Kashima. Since a station position by geodesic VLBI observations has not been measured even once for the Nobeyama 45-m antenna, a baseline vector error of about 50 cm is considered plausible and its contribution as such to total error can be calculated. The next largest contribution is the structure of the maser feature used as a positional reference. While a structure within one velocity channel is simple, the brightness distribution for all maser emission lines in the reference feature that can be observed over multiple channels is somewhat expansive. This must be taken into account when tracking the motion of a physical entity. In the observations described here, moreover, KR 143 is extremely faint, and position measurements with accuracy of 1 milliarc second or better could not be expected. Taking all of the above into consideration, we conclude that the accuracy of relative position measurement is about 2 milliarc second.

Another important consideration is that in the differential VLBI observations using fast antenna switching in a relatively high-frequency band like the 22.2-GHz band,

Table 6 Estimated contribution to error in relative VLBI observations between S Per water maser and continuum source KR 143

Thermal noise when detecting KR 143[1]	0.51 mas
Thermal noise when detecting reference maser spot[2]	0.10 mas
Structure of reference maser spot	0.65 mas
Error in baseline vector ($\sigma_D \cong 50$ cm)[3]	1.96 mas
Unreliable positions of reference maser spot ($\leq$0."1)[4] in standard coordinate system	<0.01 mas
Estimated error in excess system delay (about 0.1 nsec[5])	0.02 mas
Error in delay tracking model[6] in correlation-processing	0.02 mas
Total	2.13 mas

[1]For beam size and S/N of 7.1 mas and 7.
[2]For beam size and S/N of 4.7 mas and 23.6.
[3]Assuming a length of 200 km for the Kashima-Nobeyama baseline, the main contributor to error.
[4]Where offset of frequency including reference maser spot from band-center frequency is calculated as 1.3 MHz.
[5]For typical S/N of 60.
[6]Error according to "Δsec Z" term (Reid et al.[16], Eq. (1)), assuming that uncertainty in excess optical-path length in zenith direction is 8.6 cm and zenith angle at time of observation is 30 degrees.

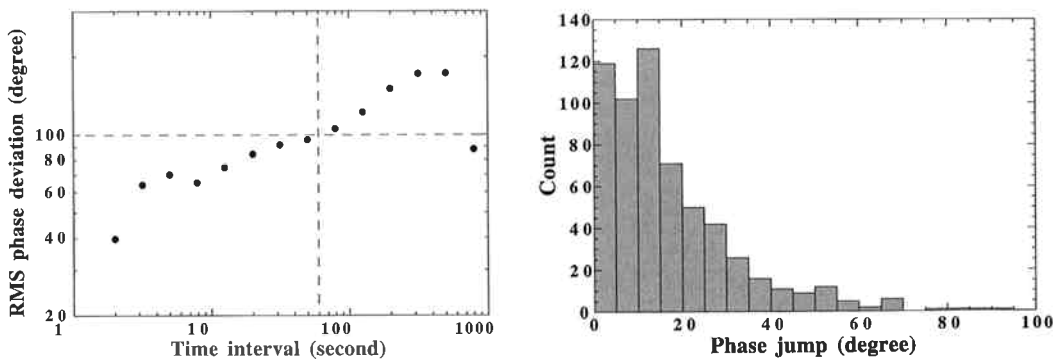

Fig. 6 Left graph: Fringe-phase structure function observed through a specific radial-velocity component of the S Per water maser.
Right graph: Frequency distribution of fringe-phase difference during consecutive 30-second scans (one-minute intervals) observed through a specific radial-velocity component of the S Per water maser.

fringe-phase fluctuation caused by the atmosphere can be effectively cancelled out. To this end, it is essential that the data obtained on the day of observation be analyzed and that the structure function, the Alla variance, etc. of the fringe phase be determined. The left graph of Fig. 6 shows the structure function of the maser-source fringe phase determined from part of the observation data. For an interval of 60 seconds, corresponding to the observation cycle, fringe-phase dispersion reaches 100 degrees, while if fringe fitting is done at three-minute intervals, the dispersion is kept to within about 30 degrees. In either case, though, we see that fringe-phase tracking is possible (no rotation above 2π radians). The right graph of Fig. 6, moreover, shows the frequency distribution of fringe-phase difference at one-minute intervals. For almost all scans, fringe phase settles within a change of 60 degrees, which shows that fringe-phase tracking is effective. In contrast, though, a 100-degree or greater change in fringe phase occurs often in the 43-GHz band or in the higher frequency bands, and this would probably lead to failure in fringe-phase tracking.

5. Summary

The following developments have occurred as a result of a sequence of water-maser observations on J-Net. (1) Radial velocity drift (acceleration?) can now be monitored in addition to the spatial motion and (assuming constant-velocity motion) proper motion of maser spots as done in the past. This is a major step forward in the understanding of gas dynamics around pulsating variable stars. (2) The discovery of rotation-infall motions of gas around a protostar (dynamical infalls) by water maser observations represents a major breakthrough in the understanding of gas dynamics near the surface of a protostar. The measurement of relative proper motion between maser features by J-Net has also become possible. At the same time, though, the accuracy of proper-motion measurements is limited to 0.1 milliarc second, which reveals the limitations of this technique based on past methods. In addition, the differential VLBI method using fast antenna switching was shown to be effective, but barely, in the 22.2 GHz band. It was seen, however, that effectiveness drops in differential VLBI observations at higher frequency bands due to fringe-phase fluctuation caused by the atmosphere, and that pairs of celestial objects for which observations can be performed by a telescopic drive are extremely limited (about 0.5 degree at maximum). These problems are expected to be overcome by the VLBI Exploration of Radio Astrometry (VERA) project now under construction by the National Astronomical Observatory featuring multiple-view differential VLBI equipment.

Acknowledgments

While this article summarizes the research achievements of J-Net VLBI observations conducted by the authors, they could not have been possible without the assistance of many people. In particular, the authors would like to extend their deep appreciation to everyone at the Radio Astronomy Applications Section of the CRL Kashima Space Research Center for granting precious observation time on the 34-m antenna and for their gracious assistance in its operation. The authors would also like to extend their sincere gratitude to those involved in J-Net operation from the National Astronomical Observatory and the Space Science Course of the Faculty of Science, Kagoshima University, and to collaborative researchers as well, for their valuable help in VLBI observations, correlation processing, data analysis, and the writing of reference works.

References

(1) Omodaka T., et al., 1994, in VLBI Technology, Progress and Future Observational Possibilities, ed T. Sasao, S. Manabe, O. Kameya, M. Inoue (Terra Scientific Publishing Company, Tokyo) p.191.
(2) Kiuchi H., et al., 1991, in Proceedings of the AGU Chapman Conference on Geodetic VLBI: Monitoring Global Change, NOAA Technical Report NOS 137, p.35.
(3) Kawaguchi N., 1991, in Frontiers of VLBI, ed H. Hirabayashi, M. Inoue, H. Kobayashi (Universal Academy Press, Tokyo) p.75.
(4) Shibata K.M., et al., 1994, in VLBI TECHNOLOGY, Progress and Future Observational Possibilities, ed T. Sasao, S. Manabe, O. Kameya, M. Inoue (Terra Scientific Publishing Company, Tokyo) p.327.
(5) Chikada Y., et al., 1991, in Frontiers of VLBI, ed H. Hirabayashi, M. Inoue, H. Kobayashi (Universal Academy Press, Tokyo) p.79.
(6) Imai H., et al., 1997, A&A, 319, L1.
(7) Fiebig D., et al., 1996, A&A, 310 199.
(8) Imai H., Iwata T., Miyoshi M., 1999, PASJ, 51, 473.
(9) Imai H., et al., 2000, ApJ, 538, 751.
(10) Ohashi N., et al., 1997, ApJ, 488, 317.
(11) Ishitsuka J.I., et al., 2000, PASJ, submitted.
(12) Watanabe T., 2001, master thesis, Kagoshima University.
(13) Schneps M.H., et al., 1981, ApJ, 249, 124.
(14) Marvel K.B., 1996, Ph. D. thesis, New Mexico State University.
(15) Fich M., 1986, AJ, 92, 787.
(16) Reid M.J. et al., 1999, ApJ, 524, 816.